Bilinearization of the generalized coupled nonlinear Schrödinger equation with variable coefficients and gain and dark-bright pair soliton solutions

Sushmita Chakraborty, Sudipta Nandy,* and Abhijit Barthakur
Department of Physics, Cotton College Guwahati, Guwahati-781001, India

(Received 14 August 2014; revised manuscript received 22 December 2014; published 24 February 2015)

We investigate coupled nonlinear Schrödinger equations (NLSEs) with variable coefficients and gain. The coupled NLSE is a model equation for optical soliton propagation and their interaction in a multimode fiber medium or in a fiber array. By using Hirota's bilinear method, we obtain the bright-bright, dark-bright combinations of a one-soliton solution (1SS) and two-soliton solutions (2SS) for an n-coupled NLSE with variable coefficients and gain. Crucial properties of two-soliton (dark-bright pair) interactions, such as elastic and inelastic interactions and the dynamics of soliton bound states, are studied using asymptotic analysis and graphical analysis. We show that a bright 2-soliton, in addition to elastic interactions, also exhibits multiple inelastic interactions. A dark 2-soliton, on the other hand, exhibits only elastic interactions. We also observe a breatherlike structure of a bright 2-soliton, a feature that become prominent with gain and disappears as the amplitude acquires a minimum value, and after that the solitons remain parallel. The dark 2-soliton, however, remains parallel irrespective of the gain. The results found by us might be useful for applications in soliton control, a fiber amplifier, all optical switching, and optical computing.

DOI: 10.1103/PhysRevE.91.023210 PACS number(s): 05.45.Yv, 42.65.Tg, 42.81.Dp

I. INTRODUCTION

After the first real breakthrough in optical communication in 1970s with the development of the InGaAsP semiconductor laser and low loss optical fibers, the most significant development was the demonstration of an optical-soliton-based communication system. It has been demonstrated both theoretically [1] as well as experimentally [2] that a suitable balance between the dispersion and the nonlinear effect can generate a stable pulse, which can propagate through a fiber as a soliton. In comparison to bright solitons, dark solitons are found to be less affected by the background noise and perturbations, and their interactions are weaker [3]. Over the past two decades there have been many significant contributions to the experimental and theoretical development of dark and bright optical soliton (see Refs. [4,5], and the references therein).

Dispersion and nonlinear effect in some cases, for example in a mode-locked fiber laser, can be so strong that the pulse parameters, namely the width, chirp, phase, and position, vary significantly from their initial values. To deal with such a problem, the concept of soliton dispersion management and soliton control in a fiber has been recently developed, that is, with a suitable combination of fibers exhibiting normal and anomalous dispersion, a stretched fiber laser can be realized that can produce a dispersion-managed pulse in the form of a soliton [4,6].

Dispersion management of a soliton is described by the standard nonlinear Schrödinger equation (NLSE) model with varying dispersion and nonlinear coefficients along with a gain or loss coefficient [7],

$$i\mathbf{q}_z + \beta\frac{D(z)}{2}\mathbf{q}_{tt} + \gamma R(z)|\mathbf{q}|^2\mathbf{q} = i\Gamma(z)\mathbf{q}, \tag{1}$$

where $\mathbf{q}(z,t)$ is a slowly varying pulse envelope in a reference frame, moving with the group velocity of the pulse, $D(z)$ and $R(z)$ represent the group velocity dispersion and nonlinearity parameters, and $\Gamma(z) = \frac{\partial_z R(z)D(z) - R(z)\partial_z D(z)}{2R(z)D(z)}$ is the gain parameter. In [7], the authors reported for the first time the existence of a dispersion managed (DM) soliton for such a system. The fundamental bright and dark soliton solutions of Eq. (1) with $\beta = \pm 1$, respectively, are

$$\mathbf{q} = \begin{cases} \eta\sqrt{\frac{D(z)}{\gamma R(z)}}\operatorname{sech}(\eta t)e^{0.5i\eta^2\int_0^z D(\zeta)d\zeta} & \text{(bright)}, \\ \eta\sqrt{\frac{D(z)}{\gamma R(z)}}\tanh(\eta t)e^{i\eta^2\int_0^z D(\zeta)d\zeta} & \text{(dark)}. \end{cases} \tag{2}$$

The fact that a DM soliton can not only be accelerated but also be amplified preserving its shape and elastic character makes it more suitable for physical applications compared to a conventional soliton. Recently, there have been many important publications based on the model (1) [7,8] and also based on a more recently developed nonautonomous soliton model [9,10], where researchers showed many new results and predicted various applications of DM solitons. For example, in [11] the authors analyzed the control of soliton velocity with a dispersion-decreasing fiber profile in the framework of a variable coefficient NLSE, and through asymptotic analysis they verified the elastic character of two soliton interaction. In [12] the authors studied the dynamics of nonlinear pulse propagation in an averaged DM soliton system by using a variable coefficient NLSE, and they showed that the Hirota bilinear method, which is a well-known method for conventional NLSEs, is also applicable to a variable coefficient NLSE. In [13] the authors reported the interaction of chirped solitons based on models described in [8]. In more recent studies, authors reported on the dynamics of a bright soliton [14,15] and a dark soliton [16] in a generalized nonautonomous NLSE model. It may be noted here that Eq. (1) also serves as a model for the Bose-Einstein condensates (BECs) but with the roles of space and time interchanged

*Author to whom all correspondence should be addressed: sudiptanandy@gmail.com

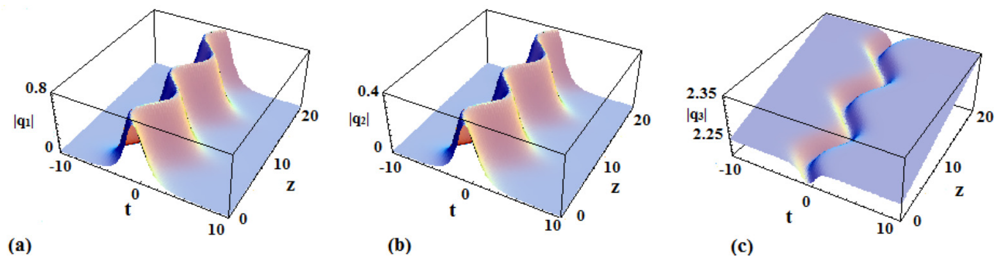

FIG. 1. (Color online) Evolution of a bright soliton in two components, $|q_1|,|q_2|$, in (a) and (b) and a dark soliton in one component, $|q_3|$, in (c) with $\gamma = 1$, $\sigma_1 = \sigma_2 = -\sigma_3 = 1$, $\eta = 1 - i$, $\zeta = 4$, $\chi = 1 + 2i$, $\alpha_{11} = 2 + i$, $\alpha_{12} = 1 - i$ and the soliton management parameters $k = \frac{\pi}{4}$, $\sigma = 0.005$, and $\Gamma(z) = 0.0025$.

and with nonlinearity management connected to the concept of the Feshbach resonance [17].

In comparison to a scalar optical soliton, a vector soliton (with more than one mutually self-trap components), proposed by Manakov [18], has many additional aspects, such as soliton propagation as bright-bright, bright-dark soliton pair in a multimode fiber [19,20], soliton propagation as coupled periodic waves with opposite dispersion in a nonlinear fiber [21], soliton interactions in two-core optical fibers [22], soliton shape-changing and intermodal energy exchange during inelastic soliton interaction [23] (which have potential applications in all optical switching devices, in long-distance communication systems using a multimode fiber medium, in construction of soliton-controlled logic gates [24–27], and in signal amplification by transferring energy from "pump" to "signal" [28]).

It is now natural to ask whether a DM vector soliton is also possible, and if so, what would be the soliton dynamics and the nature of their interaction. In addition, can concepts such as a bright-bright soliton, a bright-dark mixed-type soliton, inelastic soliton interactions, and soliton complexes described in the framework of the Manakov model also be described with a DM vector soliton. Secondly, can the rich mathematical insight and techniques available for conventional vector solitons also be used with a DM vector soliton given the fact that the fundamental equation for a DM soliton is the same NLSE, only with the modification that the dispersion coefficient and the nonlinearity coefficient are dependent on propagation distance. However, in the literature, other than a few notable papers, study in this direction is comparatively sparse. In [29] the authors studied a special case of a variable coefficient coupled NLSE with harmonic potential [self-phase-modulation (SPM) coefficient $\neq$ cross-phase-modulation (XPM) coefficient] by using a method based on the homogeneous balance principle and the F-expansion technique, and they obtained the traveling wave and soliton solution and also showed that for such a system the interaction between two solitons with opposite transverse velocities is elastic. In [30], the authors obtained the soliton solutions using a transformation between the coupled NLSE and the coupled inhomogeneous NLSE. These papers address some important aspects, such as the existence of a soliton solution in an inhomogeneous coupled NLSE system and the connection between the two types of systems. However, many other aspects, such as elastic and inelastic soliton interactions, soliton complexes (especially in a multimode system where both bright and dark solitons coexist), and the required methodology remain unaddressed or have not been discussed anywhere in the literature to the best of our knowledge. These aspects may have interesting consequences, especially in the research of all optical logic gates using solitons.

Being motivated by the above intriguing aspects of a DM vector soliton, we introduce the generalized NLSE with variable coefficients:

$$i\mathbf{q}_{j_z} + \frac{D(z)}{2}\mathbf{q}_{j_{tt}} + \gamma R(z)\sum_{l=1}^{n}\sigma_l|\mathbf{q}_l|^2\mathbf{q}_j = i\Gamma(z)\mathbf{q}_j, \qquad (3)$$

where $\mathbf{q}_j$ $(j = 1,\ldots,n)$ are complex amplitude of the jth field component of an inhomogeneous dispersive and nonlinear optical system, subscript z denotes the partial derivative with respect to normalized distance along the direction of

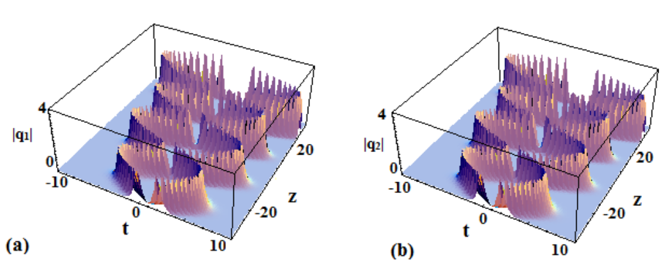

FIG. 2. (Color online) Elastic interactions between two bright solitons in (a) component $|q_1|$ and (b) component $|q_2|$ with $\gamma = 1$, $\sigma_1 = \sigma_2 = \sigma_3 = -\sigma_4 = 1$, $\eta_1 = 2 - i$, $\eta_2 = 2 + i$, $\zeta_3 = 1$, $\zeta_4 = 3$, $\chi_3 = 1 + 3i$, $\chi_4 = 1 - 3i$, and $\alpha_{11} = \alpha_{12} = \alpha_{21} = \alpha_{22} = 1$, and soliton management parameters $k = \frac{\pi}{18}$, $\sigma = 0.005$, and $\Gamma(z) = 0.0025$.

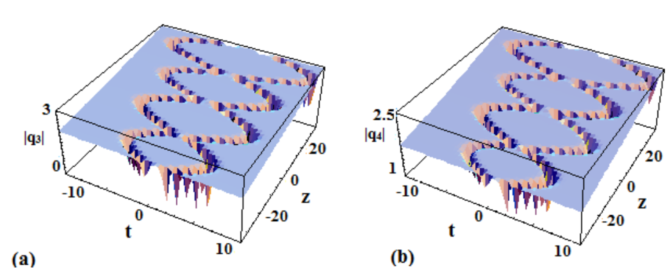

FIG. 3. (Color online) Elastic interactions between two dark solitons, component-wise, in (a) component $|q_3|$ and (b) component $|q_4|$ with $\gamma = 1$, $\sigma_1 = \sigma_2 = \sigma_3 = -\sigma_4 = 1$, $\eta_1 = 2 - i$, $\eta_2 = 2 + i$, $\zeta_3 = 1$, $\zeta_4 = 3$, $\chi_3 = 1 + 3i$, $\chi_4 = 1 - 3i$, and $\alpha_{11} = \alpha_{12} = \alpha_{21} = \alpha_{22} = 1$, and soliton management parameters $k = \frac{\pi}{18}$, $\sigma = 0.005$, and $\Gamma(z) = 0.0025$.

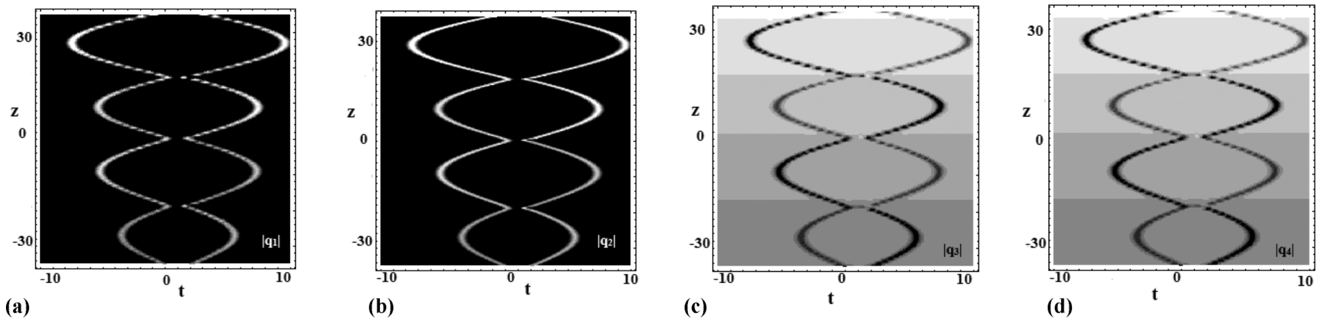

FIG. 4. Contour plot of elastic soliton interactions, component-wise, in (a) $|q_1|$, (b) $|q_2|$, (c) $|q_3|$, and (d) $|q_4|$ with the parameters as given in the caption of Figs. 2 and 3.

propagation, t denotes the partial derivative with respect to time (in a retarded frame), $D(z)$ and $R(z)$ denote the variable dispersion coefficient and the variable nonlinearity coefficient, respectively, γ stands for the strength of nonlinearity, σ_l $(=\pm 1)$ defines the sign of the nonlinearity, $\sigma_l = -1$ $(+1)$ stands for a defocusing (focusing) -type nonlinearity, and $\Gamma(z)$ is the gain coefficient and is defined in terms of $D(z)$ and $R(z)$ as $\Gamma(z) = \frac{\partial_z R(z) D(z) - R(z)\partial_z D(z)}{2R(z)D(z)}$. If $D(z)$ and $R(z)$ are two linearly independent functions, then we obtain a nonvanishing gain coefficient $(\Gamma \neq 0)$. Alternatively, if they are linearly dependent, then the gain coefficient vanishes. If $\sigma_l = +1$ (for $l = 1,2,\ldots,n$), then nonlinearity is only of a focusing type. If $\sigma_l = +1$ (for $l = 1,2,\ldots,k$) and $\sigma_l = -1$ (for $l = k+1,k+2,\ldots,n$), then both focusing (for k components) and defocusing [for $(n-k)$ components] -type nonlinearity occur at the same time.

In the framework of the model (3), we propose that a bright-bright-type soliton solution can be obtained when the bright solitons coexist in all modes with at least one $\sigma_l = +1$ (for $l = 1,2,\ldots,n$). For example, for a 2-coupled system $(n = 2)$, a bright-bright soliton can be obtained with (σ_1,σ_2) having one of the following combinations: $(1,1)$, $(1,-1)$, and $(-1,1)$. When $D(z) = R(z) = 1$, the first of the combinations, $(1,1)$, refers to the focusing-type Manakov model [18], whereas the other two combinations, $(1,-1)$ and $(-1,1)$, refer to a focusing and defocusing mixed-type model [28]. On the other hand, a bright-dark-type soliton solution with a bright soliton in k modes and a dark soliton in $(n-k)$ modes can be obtained either with $\sigma_l = -1$ (for all $l = 1,2,\ldots,n$) or with at least one $\sigma_l = +1$ (for $l = 1,2,\ldots,k$). For example, for a 3-coupled system $(n = 3)$ with a bright soliton in two modes $(l = 1,2)$ and a dark soliton in one mode $(l = 3)$, $(\sigma_1,\sigma_2,\sigma_3)$ may have any of the possible combinations $(-1,-1,-1)$, $(1,-1,-1)$, $(1,1,-1)$, $(1,-1,1)$, $(1,1,1)$, $(-1,1,-1)$, and $(-1,1,1)$. In general for an n-coupled system, a bright-bright or a bright-dark soliton may be obtained with one of the $(2^n - 1)$ possible combinations of $\sigma_1,\sigma_2,\ldots,\sigma_n$.

In the present paper, using Eq. (3) as the model equation, we will obtain the bright-bright and dark-bright one-soliton solution and two-soliton solution. We will show various cases of elastic and inelastic two-soliton interactions and two-soliton complexes in a system with a bright 2-soliton in two components and a dark 2-soliton in two components using different combinations of σ_l, presented above. To obtain the soliton solution, we will use Hirota's bilinear method [12,31–33], which is a direct and much more effective method compared to the inverse scattering method [34], since it does not require knowledge of the Lax pair. Moreover, the construction of the τ function becomes straightforward in this method. Secondly, to study the nature of soliton interaction and soliton complexes, we will depend on the asymptotic analysis as well as graphical analysis. The outcome of the analysis might be useful for realization of optical logic gates using a DM soliton.

This paper is organized as follows. Section I is the Introduction. In Sec. II, the variable coefficient coupled nonlinear Schrödinger Eq. (3) is bilinearized and a one-soliton solution as well as a two-soliton solution are obtained by using Hirota's bilinear method. In Sec. III, bright-dark mixed-type two-soliton interactions and soliton complexes are studied using asymptotic and graphical analysis. Section IV concludes the paper.

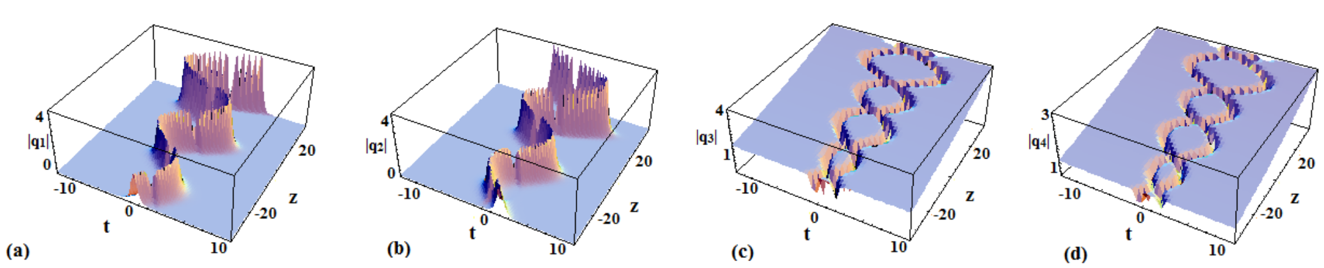

FIG. 5. (Color online) Elastic interactions between two bright solitons [in (a) $|q_1|$ and (b) $|q_2|$] and between two dark solitons [in (c) $|q_3|$ and (d) $|q_4|$]: $\gamma = 1$, $\sigma_1 = \sigma_2 = \sigma_3 = -\sigma_4 = 1$, $\eta_1 = 4 - 0.5i$, $\eta_2 = 4.1 + 0.5i$, $\zeta_3 = 4$, $\zeta_4 = 3$, $\chi_3 = 1 + 3i$, $\chi_4 = 1 - 3i$, $\alpha_{11} = \alpha_{22} = 0$, $\alpha_{12} = 2$, and $\alpha_{21} = 1$, and soliton management parameters $k = \frac{\pi}{16}$, $\sigma = 0.01$, and $\Gamma(z) = 0.005$.

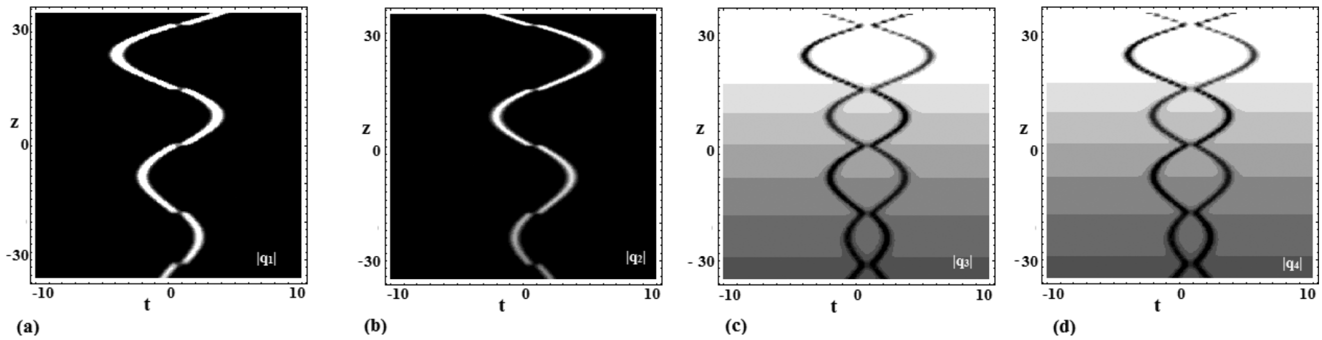

FIG. 6. Contour plot of elastic soliton interactions, component-wise, in (a) $|q_1|$, (b) $|q_2|$, (c) $|q_3|$, and (d) $|q_4|$ with the parameters as given in the caption of Fig. 5.

II. SOLITON SOLUTIONS THROUGH HIROTA'S METHOD

To write Eq. (3) in bilinear form, we make the following bilinear transformation:

$$\mathbf{q}_j = \frac{g^{(j)}(t,z)}{f(t,z)}, \tag{4}$$

where $g^{(j)}(t,z)$ is complex and $f(t,z)$ is real. Consequently, in the new set of variables we have the following set of bilinear equations:

$$\begin{aligned} &\left(iD_z + \frac{D(z)}{2}D_t^2 - \lambda\right)(g^{(j)}\cdot f) = i\Gamma(z)(g^{(j)}\cdot f),\\ &\left(\frac{D(z)}{2}D_t^2 - \lambda\right)(f\cdot f) = \gamma R(z)\sum_{l=1}^{n}\sigma_l g^{(l)}g^{(l)*}, \end{aligned} \tag{5}$$

where D_z and D_t^2 are Hirota derivatives [31] that are defined by

$$D_z^m D_t^n u(z,t)\cdot v(z,t) = \left(\frac{\partial}{\partial z} - \frac{\partial}{\partial z'}\right)^m \left(\frac{\partial}{\partial t} - \frac{\partial}{\partial t'}\right)^n \times u(z,t)v(z',t')|z' = z, t' = t.$$

To obtain the soliton solutions, $g^{(j)}$ $(j = 1,2,\ldots,k)$, $g^{(l)}$ $(l = k+1,\ldots n)$, and f are expanded with respect to an arbitrary parameter ϵ as follows:

$$\begin{aligned} g^{(j)} &= \epsilon g_1^{(j)} + \epsilon^3 g_3^{(j)} + \cdots,\\ g^{(l)} &= g_0^{(l)}(1 + \epsilon^2 g_2^{(l)} + \cdots),\\ f &= 1 + \epsilon^2 f_2 + \cdots. \end{aligned} \tag{6}$$

A. Bright 1SS in k components and dark 1SS in $(n-k)$ components

To obtain a one-soliton solution (1SS) of Eq. (3), the series (6) is truncated at ϵ^2, such that the expression for the bright-dark 1SS becomes

$$\begin{aligned} q_j &= \frac{g_1^{(j)}}{1+f_2} \quad (\text{for} \quad j = 1,2,\ldots,k),\\ q_l &= \frac{g_0^{(l)}(1+g_2^{(l)})}{1+f_2} \quad (\text{for} \quad l = k+1,\ldots,n). \end{aligned} \tag{7}$$

Let us consider

$$\begin{aligned} g_1^{(j)} &= \alpha_1^{(j)}(z)e^{\theta_1}, \quad g_0^{(l)} = \chi^{(l)}(z)e^{\phi_1},\\ g_2^{(l)} &= \kappa_1 e^{\theta_1+\theta_1^*}, \quad f_2 = \tau_1 e^{\theta_1+\theta_1^*}. \end{aligned} \tag{8}$$

Substituting Eqs. (7) and (8) into Eq. (5), we obtain the k-bright–$(n-k)$-dark 1SS, where the parameters are given by

$$\alpha_1^{(j)}(z) = \alpha_{j1}\sqrt{\frac{D(z)}{\gamma R(z)}}, \quad \chi^{(l)}(z) = \chi^{(l)}\sqrt{\frac{D(z)}{\gamma R(z)}},$$

$$\theta_1 = \frac{i\eta^2}{2}\int_0^z D(z)dz + \eta t - i\lambda z,$$

$$\phi_1 = \frac{-i\zeta^2}{2}\int_0^z D(z)dz + i\zeta t - i\lambda z,$$

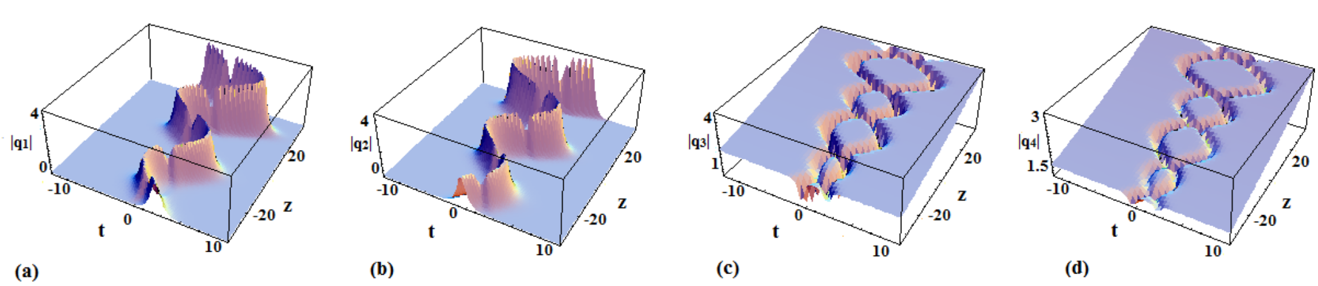

FIG. 7. (Color online) Elastic interactions between two bright solitons [in (a) $|q_1|$ and (b) $|q_2|$] and between two dark solitons [in (c) $|q_3|$ and (d) $|q_4|$] with $\gamma = 1, \sigma_1 = \sigma_2 = \sigma_3 = -\sigma_4 = 1, \eta_1 = 4+i, \eta_2 = 4.1+i, \zeta_3 = 4, \zeta_4 = 3, \chi_3 = 1+3i, \chi_4 = 1-3i, \alpha_{12}, \alpha_{21} = 0, \alpha_{11} = 4$, and $\alpha_{22} = 1$, and soliton management parameters $k = \frac{\pi}{18}, \sigma = 0.01$, and $\Gamma(z) = 0.005$.

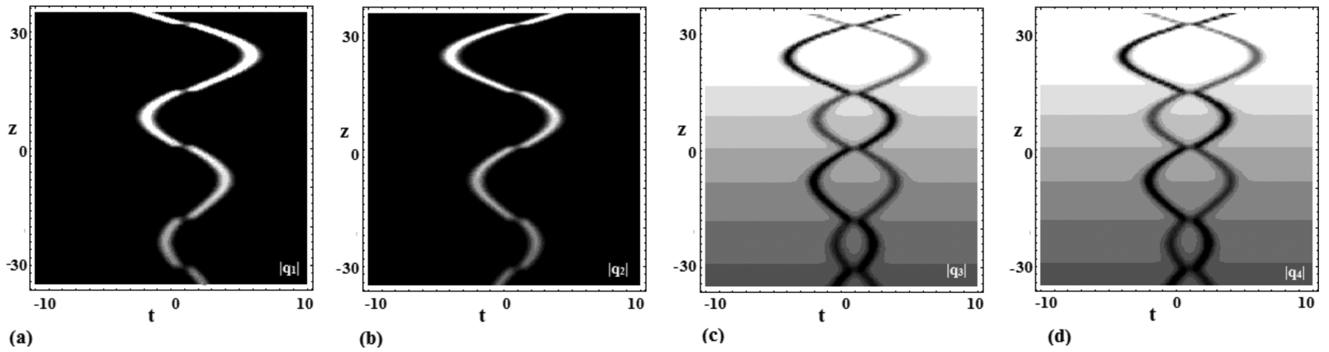

FIG. 8. Contour plot of elastic soliton interactions, component-wise, in (a) $|q_1|$, (b) $|q_2|$, (c) $|q_3|$, and (d) $|q_4|$ with the parameters as given in the caption of Fig. 7.

$$\lambda = -\gamma R(z) \sum_{l=k+1}^{n} \sigma_l |\chi^{(l)}(z)|^2, \quad \kappa_1 = \tau_1 \frac{\zeta + i\eta}{\zeta - i\eta^*},$$

$$\tau_1 = \frac{\gamma R(z)\left(\sum_{l=1}^{k} \sigma_l \left|\alpha_l^1(z)\right|^2\right)|\zeta + i\eta|^2}{(\eta+\eta^*)^2[D(z)|\zeta + i\eta|^2 - \lambda]}. \tag{9}$$

The vector DM soliton parameters given in Eq. (9) show that by choosing $\alpha_1^{(j)}(z)$ and $D(z)$, a vector DM soliton can be amplified and accelerated without changing the soliton width. This is a property similar to the scalar DM soliton only with the modification that the amplitude is now a vector, which is interesting but not surprising. If $(j = 1)$ and $(l = 0)$, the vector DM soliton Eqs. (7)–(9) reduce to a scalar bright soliton [Eq. (2)]. For a better understanding of the soliton dynamics, we use MATHEMATICA software and plot the solution (7) with $j = 1,2$ and $l = 3$. To plot the figures, we have chosen $D(z)$ and $R(z)$ as two linearly independent functions, for example $D(z) = e^{\sigma z}\cos(kz)$ and $R(z) = \cos(kz)$, such that the gain coefficient $\Gamma(z)$ $(=\sigma)$ is nonvanishing. It goes to zero only in the limit $\sigma = 0$. Figure 1 shows the soliton dynamics of bright and dark solitons component-wise, with the bright soliton in two components and the dark soliton in one component. It shows that, boosted with gain, the soliton in each component is accelerated and retarded periodically. However, for a complete knowledge of DM vector soliton properties, we need to study its particlelike behavior.

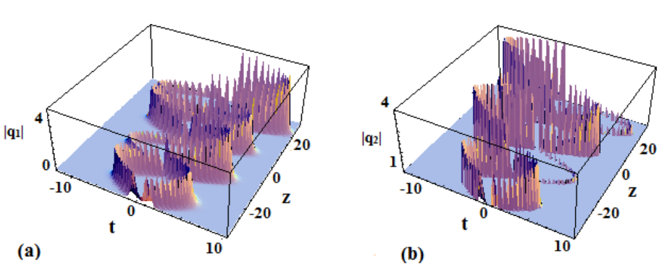

FIG. 9. (Color online) Inelastic interactions between two bright solitons in two components, $|q_1|$ in (a) and $|q_2|$ in (b), with $\gamma = 1$, $\sigma_1 = \sigma_2 = -\sigma_3 = \sigma_4 = 1$, $\eta_1 = 4 + i$, $\eta_2 = 4.1 + i$, $\zeta_3 = 4$, $\zeta_4 = 3$, $\chi_3 = 1 + 3i$, $\chi_4 = 1 - 3i$, $\alpha_{11} = \alpha_{12} = \alpha_{21} = 1$, and $\alpha_{22} = 8$, and soliton management parameters $k = \frac{\pi}{18}$, $\sigma = 0.005$, and $\Gamma(z) = 0.0025$.

B. Bright 2SS in k components and dark 2SS in $(n-k)$ components

A two-soliton solution of Eq. (3) is obtained with the series (6) truncated at ϵ^4. The expression for the bright-dark pair soliton is then given by

$$q_j = \frac{g_1^{(j)} + g_3^{(j)}}{1 + f_2 + f_4}, \quad q_l = \frac{g_0^{(l)}\left(1 + g_2^{(l)} + g_4^{(l)}\right)}{1 + f_2 + f_4} \tag{10}$$

(for $j = 1,2,\ldots,k$ and $l = k+1,k+2,\ldots,n$).

Now by choosing j and l, we may obtain a class of bright-bright and bright-dark mixed-type two-soliton solutions. For example, (i) with the choice $j = 1,2, l = 3$, and by substituting Eq. (10) in Eq. (5), we obtain a two-soliton solution, where the bright 2-soliton is in components 1 and 2 and the dark 2-soliton is in component 3 [see solution (A1) in the Appendix]. (ii) Again with the choice $j = 1,2$, $l = 3,4$, and substituting Eq. (10) in Eq. (5), we obtain another example of a two-soliton solution, where a bright 2-soliton is in components 1 and 2 and a dark 2-soliton is in components 3 and 4 [see solution (A2) in the Appendix]. We may note that a bright-bright 2-soliton may be obtained from Eq. (10) with $j = 1,2\ldots,n$ and $l = 0$, and with the choice $j = 1, l = 0$ the solution reduces to the bright 2-soliton solution of a scalar inhomogeneous NLSE [11].

III. SOLITON INTERACTION AND ASYMPTOTIC ANALYSIS

In a scalar inhomogeneous NLSE model, the velocity of the soliton changes according to the functions $D(z)$, that is, if $D(z)$ is a periodic function, then bound states are

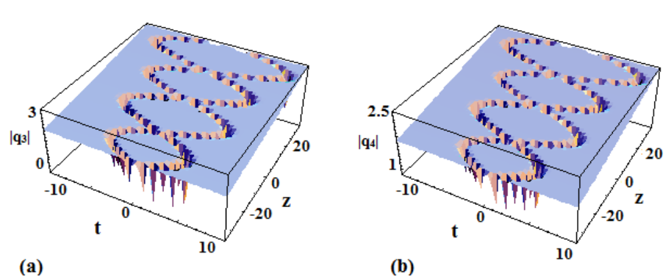

FIG. 10. (Color online) Elastic interactions between two dark solitons in two components, $|q_3|$ in (a) and $|q_4|$ in (b), with the same values of the parameters as given in the caption of Fig. 9.

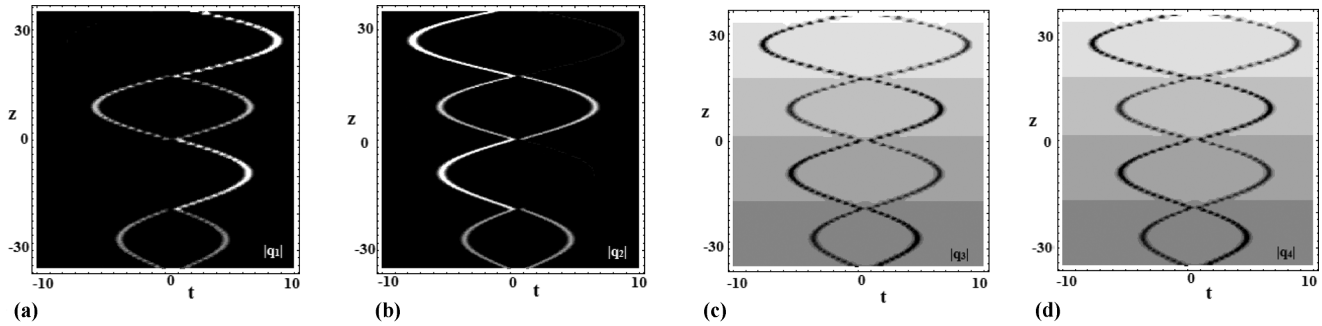

FIG. 11. Contour plot of component-wise inelastic bright soliton interactions in (a) $|q_1|$ and (b) $|q_2|$, and elastic dark soliton interaction in (c) $|q_3|$ and (d) $|q_4|$, with the parameters as given in the captions of Figs. 9 and 10.

formed periodically, as explained in [7,8]. However, in a multicomponent system, soliton interaction has additional aspects.

To understand the interaction explicitly, let us analyze the asymptotic behavior of the two-soliton solution (10). Let us consider a 4-coupled system with a bright soliton in two modes, with $j = 1,2$, and a dark soliton in two modes, with $l = 3,4$ [see solution (A2) in the Appendix]. Variable coefficients $D(z)$ and $R(z)$ are chosen to be two linearly independent functions, namely $D(z) = e^{\sigma z}\cos(kz)$ and $R(z) = \cos(kz)$. When $\sigma = 0$, two functions become linearly dependent (that is, zero gain). The asymptotic limit is obtained when the solitons are sufficiently apart such that there is no interaction between them. Thus, asymptotically as $z \to -\infty$,

$$\begin{aligned} q_1^{(j)}|^- &= \frac{\alpha_{j1}\sqrt{\frac{D(z)}{\gamma R(z)}}e^{\theta_1}}{1+\tau_1 e^{\theta_1+\theta_1^*}}, \\ q_1^{(l)}|^- &= \frac{\chi^{(l)}\sqrt{\frac{D(z)}{\gamma R(z)}}e^{\phi^{(l)}}\left(1+\kappa_1^{(l)}e^{\theta_1+\theta_1^*}\right)}{1+\tau_1 e^{\theta_1+\theta_1^*}} \end{aligned} \tag{11}$$

for $(\theta_2+\theta_2^* \to -\infty)$, and

$$\begin{aligned} q_2^{(j)}|^- &= \frac{l_{j1}e^{\theta_2}}{\tau_1+\varrho e^{\theta_2+\theta_2^*}}, \\ q_2^{(l)}|^- &= \frac{\chi^{(l)}\sqrt{\frac{D(z)}{\gamma R(z)}}e^{\phi^{(l)}}\left(\kappa_1^{(l)}+\rho^{(l)}e^{\theta_2+\theta_2^*}\right)}{\tau_1+\varrho e^{\theta_2+\theta_2^*}} \end{aligned} \tag{12}$$

for $(\theta_1+\theta_1^* \to +\infty)$.

As $z \to +\infty$,

$$\begin{aligned} q_1^{(j)}|^+ &= \frac{l_{j2}e^{\theta_1}}{\tau_4+\varrho e^{\theta_1+\theta_1^*}}, \\ q_1^{(l)}|^+ &= \frac{\chi^{(l)}\sqrt{\frac{D(z)}{\gamma R(z)}}e^{\phi^{(l)}}\left(\kappa_4^{(l)}+\rho^{(l)}e^{\theta_1+\theta_1^*}\right)}{\tau_4+\varrho e^{\theta_1+\theta_1^*}} \end{aligned} \tag{13}$$

for $(\theta_2+\theta_2^* \to +\infty)$, and

$$\begin{aligned} q_2^{(j)}|^+ &= \frac{\alpha_{j2}\sqrt{\frac{D(z)}{\gamma R(z)}}e^{\theta_2}}{1+\tau_4 e^{\theta_2+\theta_2^*}}, \\ q_2^{(l)}|^+ &= \frac{\chi^{(l)}\sqrt{\frac{D(z)}{\gamma R(z)}}e^{\phi^{(l)}}\left(1+\kappa_4^{(l)}e^{\theta_2+\theta_2^*}\right)}{1+\tau_4 e^{\theta_2+\theta_2^*}} \end{aligned} \tag{14}$$

for $(\theta_1+\theta_1^* \to -\infty)$, where $(j = 1,2)$ and $(l = 3,4)$.

Let $\mathcal{A}_j^{1-}$, $\mathcal{A}_j^{2-}$ denote the amplitudes and let Φ_j^{1-}, Φ_j^{2-} denote the phases of soliton 1 and soliton 2, respectively, before interaction, and let $\mathcal{A}_j^{1+}$,$\mathcal{A}_j^{2+}$ denote the amplitudes and Φ_j^{1+},Φ_j^{2+} denote the phases of the same two solitons after interaction. Then under one of the following conditions:

$$\left|\frac{\alpha_1^{(1)}(z)}{\alpha_1^{(2)}(z)}\right| = \left|\frac{\alpha_2^{(1)}(z)}{\alpha_2^{(2)}(z)}\right|, \tag{15}$$

$$\alpha_1^{(1)}(z),\alpha_2^{(2)}(z) = 0; \quad \alpha_2^{(1)}(z) \neq 0; \quad \alpha_1^{(2)}(z) \neq 0; \tag{16}$$

$$\alpha_2^{(1)}(z),\alpha_1^{(2)}(z) = 0; \quad \alpha_1^{(1)}(z) \neq 0; \quad \alpha_2^{(2)}(z) \neq 0; \tag{17}$$

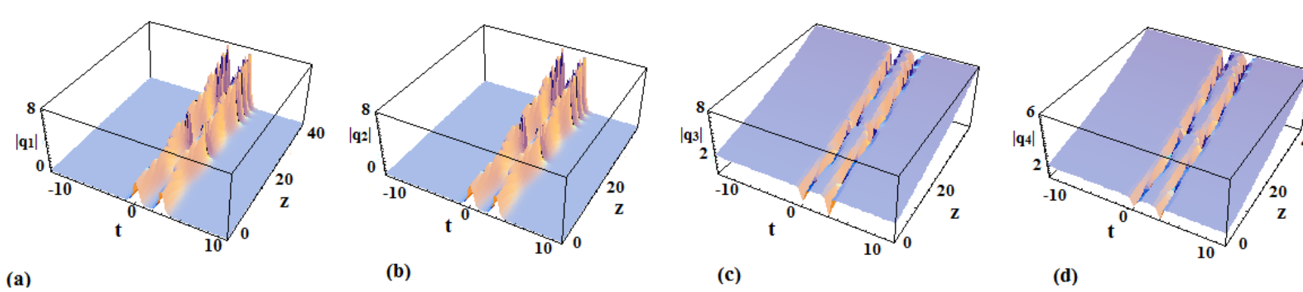

FIG. 12. (Color online) Soliton complexes of bright 2-solitons [in (a) $|q_1|$ and (b) $|q_2|$] and of dark 2-solitons [in (c) $|q_3|$ and (d) $|q_4|$] with $\gamma = 1, \sigma_1 = \sigma_2 = \sigma_3 = \sigma_4 = 1, \eta_1 = 4, \eta_2 = 4.1, \zeta_3 = 1, \zeta_4 = 3, \chi_3 = 1+3i, \chi_4 = 1-2i$, and $\alpha_{11} = \alpha_{22} = \alpha_{12} = \alpha_{21} = 1$, and soliton management parameters $k = \frac{\pi}{18}$, $\sigma = 0.05$, and $\Gamma(z) = 0.025$.

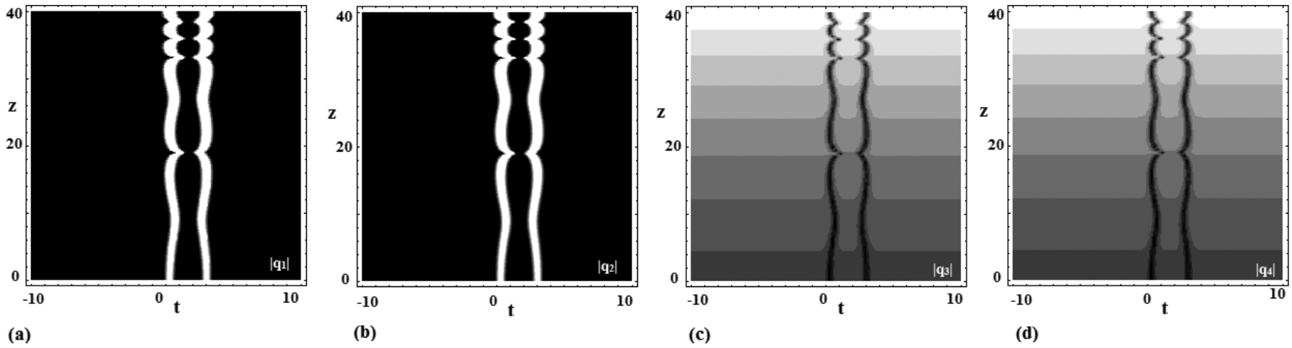

FIG. 13. Contour plot of 2-soliton complexes, component-wise, in (a) $|q_1|$, (b) $|q_2|$, (c) $|q_3|$, and (d) $|q_4|$ with the parameters as given in the caption of Fig. 12.

we obtain

$$\mathcal{A}_j^{1-} = \mathcal{A}_j^{1+} \quad \text{and} \quad \mathcal{A}_j^{2-} = \mathcal{A}_j^{2+}. \tag{18}$$

That is, the amplitudes of the solitons remain the same before and after interaction, which is the case of an elastic interaction. However, each soliton suffers a phase shift due to interaction, that is, $\Phi_j^{1-} \neq \Phi_j^{1+}$. Figures 2 and 3 show an example of elastic interactions between two bright solitons moving with different velocities in components $|q_1|$ and $|q_2|$ and between two dark solitons in components $|q_3|$ and $|q_4|$, with $\alpha_1^{(1)}(z)$, $\alpha_1^{(2)}(z)$, $\alpha_2^{(1)}(z)$, and $\alpha_2^{(2)}(z)$ satisfying condition (18). Two solitons are periodically accelerated and retarded, and as a result they interact at a regular interval. After each interaction, the amplitude of each soliton remains the same in all the components but the phase changes. However, after two successive interactions, the net phase shift of each soliton turns out to be zero. Figure 4 shows the component-wise contour plot of the soliton interactions, shown in Figs. 2 and 3. Brighter lines in the contour plot indicate solitons with higher amplitude and darker lines indicate a dip in the amplitude in a brighter background.

A special case of elastic interaction is obtained when one bright soliton in each component vanishes asymptotically, however Eq. (18) is still satisfied. Figures 5–7 show an example of such interactions between two bright and two dark solitons with $\alpha_1^{(1)}(z)$, $\alpha_1^{(2)}(z)$, $\alpha_2^{(1)}(z)$, and $\alpha_2^{(2)}(z)$ satisfying either of the conditions given in Eqs. (16) and (17). One of the solitons in each component vanishes asymptotically, and only one soliton figures in components $|q_1|$ and $|q_2|$. However, a phase shift is still observed after each interaction, but the net phase shift of each soliton after two consecutive interactions is always zero. Figures 6–8 show the component-wise contour plot of the soliton dynamics shown in Figs. 5–7, respectively.

On the other hand, if none of the conditions in Eqs. (15)–(17) is satisfied, then we obtain

$$\mathcal{A}_j^{1-} \neq \mathcal{A}_j^{1+} \quad \text{and} \quad \mathcal{A}_j^{2-} \neq \mathcal{A}_j^{2+} \tag{19}$$

and the interaction is an inelastic interaction, and then shape-changing phenomena and energy exchange between the soliton components are noticed. However, dark soliton interactions are always found to be elastic. Figure 9 shows an example of inelastic interactions between two bright solitons in components $|q_1|$ and $|q_2|$ moving with different velocities, and Fig. 10 displays the elastic interactions between two dark solitons in components $|q_3|$ and $|q_4|$ moving with different velocities, with $\alpha_1^{(1)}(z)$, $\alpha_1^{(2)}(z)$, $\alpha_2^{(1)}(z)$, and $\alpha_2^{(2)}(z)$ satisfying the condition (19). In component $|q_1|$, after an interaction, one of the solitons (say soliton "1") gains energy at the expanse of the energy of the other (say soliton "2"). In component $|q_2|$, after interaction, soliton "2" recovers the parted energy and soliton "1" sheds energy. In addition to that during the interaction, solitons also suffer a phase shift. The exchange of energy and phase-shift are only temporary, and during the subsequent interaction, again there is an exchange of energy combined with a phase shift, but on this occasion the inelastic interaction exactly compensated the energy transfer, and phase shift occurred in the preceding interaction. That is, the net intercomponent energy transfer and soliton phase shift after two successive interactions are zero, which is different from the inelastic interaction in a Manakov two-soliton interaction [23], where the velocity and the amplitude of the soliton are both constant. This is interesting, and we may describe this as if an

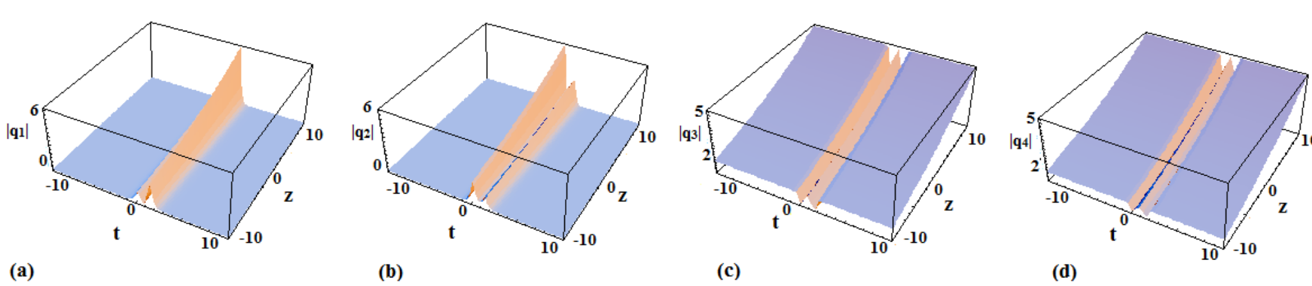

FIG. 14. (Color online) Soliton complexes of bright 2-solitons [in (a) $|q_1|$ and (b) $|q_2|$] and of dark 2-soliton [in (c) $|q_3|$ and (d) $|q_4|$], with $\gamma = 1, \sigma_1 = \sigma_2 = \sigma_3 = \sigma_4 = 1, \eta_1 = 4, \eta_2 = 4.1, \zeta_3 = 1, \zeta_4 = 3, \chi_3 = 1 + 3i, \chi_4 = 1 - 2i, \alpha_{11} = 1, \alpha_{22} = 2$, and $\alpha_{12} = \alpha_{21} = 0$, and soliton management parameters $k = \frac{\pi}{18}$, $\sigma = 0.05$, and $\Gamma(z) = 0.025$.

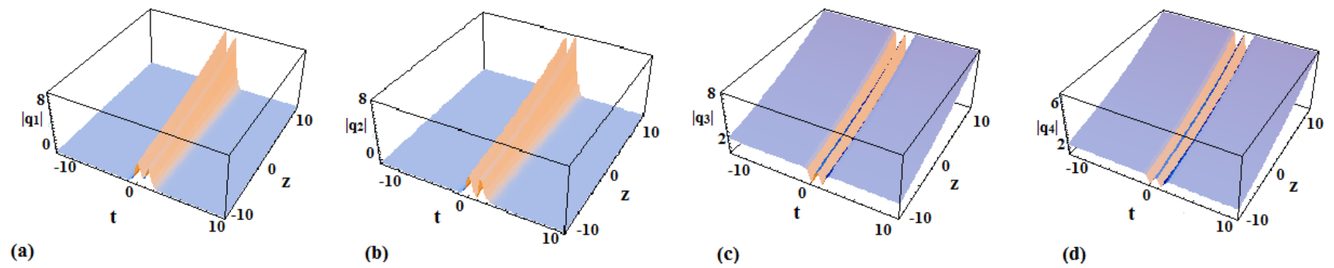

FIG. 15. (Color online) Soliton complexes of a bright 2-soliton [in (a) $|q_1|$ and (b) $|q_2|$] and of dark 2-solitons [in (c) $|q_3|$ and (d) $|q_4|$] with $\gamma = 1$, $\sigma_1 = \sigma_2 = \sigma_3 = -\sigma_4 = 1$, $\gamma = 1$, $\eta_1 = 4$, $\eta_2 = 4.1$, $\zeta_3 = 1$, $\zeta_4 = 3$, $\chi_3 = 1 + 3i$, $\chi_4 = 1 - 2i$, $\alpha_{12} = 1$, $\alpha_{21} = 2$, and $\alpha_{11} = \alpha_{22} = 0$, and soliton management parameters $k = \frac{\pi}{18}$, $\sigma = 0.05$, and $\Gamma(z) = 0.025$.

input signal is passing through two successive "NOT" gates and ultimately remained unchanged. Dark solitons, however, do not exhibit inelastic interaction; only a phase shift is noticed after each interaction. The net soliton phase shift after two successive interactions is again zero. Figure 11 shows the component-wise contour plot of the soliton dynamics shown in Figs. 9 and 10.

In a bound state, two interacting solitons, moving with the same velocity (or no relative velocity), do not move away sufficiently apart from each other, and hence asymptotic analysis does not apply here. Figures 12–17 display different cases of bound 2-solitons obtained under different conditions. Figure 12 shows the bound state of a bright 2-soliton in components $|q_1|$ and $|q_2|$ and a dark 2-soliton in components $|q_3|$ and $|q_4|$, with α_{11}, α_{12}, α_{21}, and α_{22} chosen arbitrarily. In all the components, solitons mutually attract and repel each other but the interval of their attraction increases with "z" [because of gain of the medium $\Gamma(z)$], and at "$-z$" the intensity of solitons falls to such a level so that there is no attraction and repulsion between them and they remain parallel to each other, whereas in [1,5,26] the normal scalar and vector solitons mutually interact via attraction and repulsion at regular (z) intervals. However, such interactions may have an adverse effect on an optical communication system, as reported in [22]. Figure 13 shows the component-wise contour plot of the soliton complexes shown in Fig. 12.

Figures 14 and 15 show the dynamics of a bound 2-soliton when the conditions Eqs. (16) and (17) are satisfied, respectively (Fig. 14 with $\alpha_{11} = 1$, $\alpha_{12} = 0$, $\alpha_{21} = 0$, and $\alpha_{22} = 2$ and Fig. 15 with $\alpha_{11} = 0$, $\alpha_{12} = 1$, $\alpha_{21} = 2$, and $\alpha_{22} = 0$). Two bright solitons in components $|q_1|$ and $|q_2|$ and two dark solitons in components $|q_3|$ and $|q_4|$ just remain parallel to each other without any interaction (attraction or repulsion) even if the solitons overlap. The gain of the medium makes no impact on the interaction profile.

We obtained an interesting breatherlike structure of soliton complexes when one of the following conditions is satisfied. (i) $\alpha_{11} = -\alpha_{21}$, $\alpha_{12} = \alpha_{22}$; (ii) $\alpha_{11} = \alpha_{21}$, $\alpha_{12} = -\alpha_{22}$; (iii) $\alpha_{11}^* = \alpha_{22}$, $\alpha_{12} = -\alpha_{21}^*$; (iv) $\alpha_{11}^* = -\alpha_{22}$, $\alpha_{12} = \alpha_{21}^*$. Figure 16 demonstrates a breatherlike bright 2-soliton, breathing alternately in components $|q_1|$ and $|q_2|$, and a normal dark 2-soliton in $|q_3|$ and $|q_4|$. In component $|q_1|$, one of the solitons maintains a smoother profile compared to the other, whereas in component $|q_2|$ the role is just reversed; however, solitons breath faster with increasing z [because of gain $\Gamma(z)$]. The dark 2-solitons in components $|q_3|$ and $|q_4|$ just move parallel to each other as two overlapping solitons. Figure 17 shows the component-wise contour plot of the soliton complexes shown in Fig. 16.

From the above analysis, it is interesting to note that in two-soliton complexes, even though two solitons are not involved in any collision, the presence of one may influence properties such as the velocity and energy distribution of the other soliton. These may have interesting consequences in the higher-order soliton, when a two-soliton complex interacts with another soliton. Furthermore, the analysis also reveals that compared to dark solitons, bright solitons are more responsive to interactions and exhibit many interesting behaviors, as shown in Figs. 12–17, which might be useful in soliton control and all optical switching devices. Dark solitons, however, may be more useful for optical communications because of their indifferent nature in interactions.

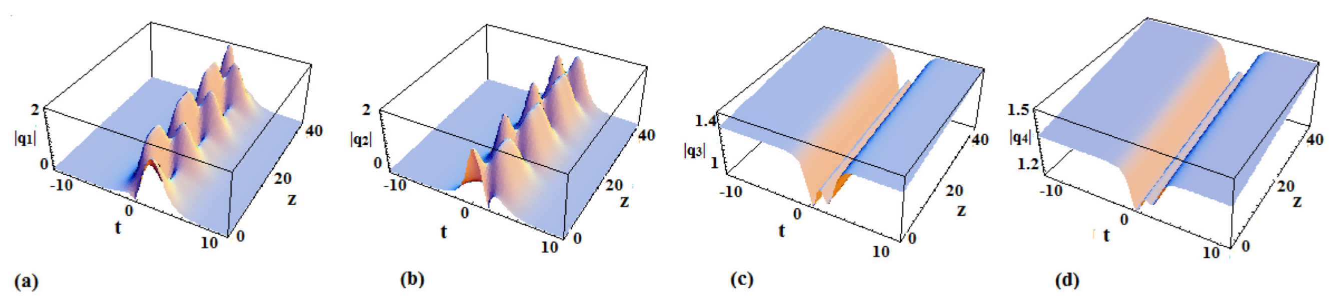

FIG. 16. (Color online) Breatherlike bright 2-soliton [in (a) $|q_1|$ and (b) $|q_2|$] and of normal dark 2-solitons [in (c) $|q_3|$ and in (d) $|q_4|$] with $\gamma = 1$, $\sigma_1 = \sigma_2 = \sigma_3 = -\sigma_4 = 1$, $\eta_1 = 1$, $\eta_2 = 1.6$, $\zeta_3 = 1$, $\zeta_4 = 3$, $\chi_3 = 1 + i$, $\chi_4 = 1 - i$, $\alpha_{21} = -1$, and $\alpha_{11} = \alpha_{22} = \alpha_{12} = 1$, and soliton management parameters $k = \frac{\pi}{12}$, $\sigma = 0.005$, and $\Gamma(z) = 0.0025$.

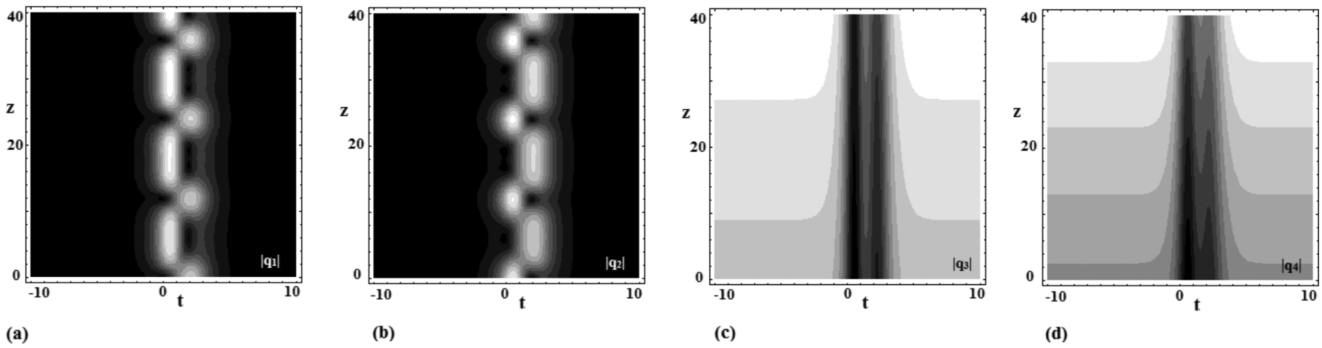

FIG. 17. Contour plot of 2-soliton complexes, component-wise, in (a) $|q_1|$, (b) $|q_2|$, (c) $|q_3|$, and (d) $|q_4|$ with the parameters as given in the caption of Fig. 16.

IV. CONCLUSION

We have studied the inhomogeneous coupled NLSE with variable dispersion, nonlinear, and gain coefficients through Hirota's bilinear method. Bright-dark soliton interactions and the soliton complexes are studied by asymptotic and graphical analysis. Interesting shape-changing phenomena, associated with energy exchanges between the bright soliton components, are noticed under specific conditions. We have also studied the soliton complexes through asymptotic and graphical analysis, and we found that two comoving solitons of sufficient amplitude (width-inverse) are subjected to periodic attraction and repulsion, and under a specialized condition the solitons demonstrate a breatherlike structure and all such processes become faster with gain. The analysis done in this paper might be useful for the development of all optical communication systems, soliton control, switching devices, and logic gates. The analysis for a 2-soliton in two components can be straightforwardly generalized to an N-soliton in n components.

ACKNOWLEDGMENT

The authors are grateful to Rajarshee Roy for fruitful discussion and fruitful suggestions.

APPENDIX

A bright 2-soliton is in components 1 and 2 and a dark 2-soliton is in component 3,

$$q_j = \frac{g_1^{(j)} + g_3^{(j)}}{1 + f_2 + f_4} \quad (\text{for} \quad j = 1,2),$$
$$q_3 = \frac{g_0^{(3)}\left(1 + g_2^{(3)} + g_4^{(3)}\right)}{1 + f_2 + f_4}, \tag{A1}$$

where

$$g_1{}^{(j)} = \alpha_1^{(j)}(z)e^{\theta_1} + \alpha_2^{(j)}(z)e^{\theta_2},$$

$$g_3{}^{(j)} = l_{j1}e^{\theta_1+\theta_1{}^*+\theta_2} + l_{j2}e^{\theta_1+\theta_2+\theta_2{}^*},$$
$$g_0{}^{(3)} = \chi^{(3)}(z)e^{\phi(3)},$$
$$g_2{}^{(3)} = \kappa_1^{(3)}e^{\theta_1+\theta_1{}^*} + \kappa_2^{(3)}e^{\theta_2+\theta_1{}^*} + \kappa_3^{(3)}e^{\theta_1+\theta_2{}^*} + \kappa_4^{(3)}e^{\theta_2+\theta_2{}^*},$$

$$g_4{}^{(3)} = \rho^{(3)}e^{\theta_1+\theta_1{}^*+\theta_2+\theta_2{}^*},$$
$$f_2 = \tau_1 e^{\theta_1+\theta_1{}^*} + \tau_2 e^{\theta_2+\theta_1{}^*} + \tau_3 e^{\theta_1+\theta_2{}^*} + \tau_4 e^{\theta_2+\theta_2{}^*},$$
$$f_4 = \varrho e^{\theta_1+\theta_1{}^*+\theta_2+\theta_2{}^*},$$

$$\theta_1 = i\frac{\eta_1{}^2}{2}\int D(z)dz + \eta_1 t - i\lambda z,$$
$$\theta_2 = i\frac{\eta_2{}^2}{2}\int D(z)dz + \eta_2 t - i\lambda z,$$
$$\alpha_1^{(j)}(z) = \alpha_{1j}\sqrt{\frac{D(z)}{\gamma R(z)}}, \quad \alpha_2^{(j)}(z) = \alpha_{2j}\sqrt{\frac{D(z)}{\gamma R(z)}},$$
$$\chi^{(3)}(z) = \chi^{(3)}\sqrt{\frac{D(z)}{\gamma R(z)}}, \quad \lambda = -\gamma R(z)\sigma_3|\chi^{(3)}(z)|^2,$$
$$\phi^{(3)} = -i\frac{\zeta_3{}^2}{2}\int D(z)dz + i\zeta_3 t - i\lambda z,$$

$$l_{j1} = (\eta_1 - \eta_2)\sqrt{\frac{D(z)}{\gamma R(z)}}\left[\frac{\alpha_{j1}\tau_2}{\eta_1 + \eta_1{}^*} - \frac{\alpha_{j2}\tau_1}{\eta_2 + \eta_1{}^*}\right],$$
$$l_{j2} = (\eta_1 - \eta_2)\sqrt{\frac{D(z)}{\gamma R(z)}}\left[\frac{\alpha_{j1}\tau_4}{\eta_1 + \eta_2{}^*} - \frac{\alpha_{j2}\tau_3}{\eta_2 + \eta_2{}^*}\right],$$
$$\rho = \varrho\frac{(\zeta_3 + i\eta_1)(\zeta_3 + i\eta_2)}{(\zeta_3 - i\eta_2{}^*)(\zeta_3 - i\eta_1{}^*)},$$
$$\varrho = |\eta_1 - \eta_2|^2\left[\frac{\tau_1\tau_4}{|\eta_1 + \eta_2{}^*|^2} - \frac{\tau_2\tau_3}{(\eta_2 + \eta_2{}^*)(\eta_1 + \eta_1{}^*)}\right],$$

$$\tau_1 = \frac{\gamma R(z)\left(\sum_{j=1}^{2}\sigma_j\left|\alpha_j^1(z)\right|^2\right)(\zeta_3 + i\eta_1)(\zeta_3 - i\eta_1{}^*)}{(\eta_1 + \eta_1{}^*)^2[D(z)(\zeta_3 + i\eta_1)(\zeta_3 - i\eta_1{}^*) + \gamma R(z)\sigma_3|\chi^{(3)}(z)|^2]}, \quad \kappa_1^{(3)} = \tau_1\frac{\zeta_3 + i\eta_1}{\zeta_3 - i\eta_1{}^*},$$

$$\tau_2 = \frac{\gamma R(z)\left[\sigma_1\alpha_1^1(z)^*\alpha_1^2(z) + \sigma_2\alpha_2^1(z)^*\alpha_2^2(z)\right](\zeta_3 + i\eta_2)(\zeta_3 - i\eta_1{}^*)}{(\eta_2 + \eta_1{}^*)^2[D(z)(\zeta_3 + i\eta_2)(\zeta_3 - i\eta_1{}^*) + \gamma R(z)\sigma_3|\chi^{(3)}(z)|^2]}, \quad \kappa_2^{(3)} = \tau_2\frac{\zeta_3 + i\eta_2}{\zeta_3 - i\eta_1{}^*},$$
$$\tau_3 = \frac{\gamma R(z)\left[\sigma_1\alpha_1^2(z)^*\alpha_1^1(z) + \sigma_2\alpha_2^2(z)^*\alpha_2^1(z)\right](\zeta_3 + i\eta_1)(\zeta_3 - i\eta_2{}^*)}{(\eta_1 + \eta_2{}^*)^2[D(z)(\zeta_3 + i\eta_1)(\zeta_3 - i\eta_2{}^*) + \gamma R(z)\sigma_3|\chi^{(3)}(z)|^2]}, \quad \kappa_3^{(3)} = \tau_3\frac{\zeta_3 + i\eta_1}{\zeta_3 - i\eta_2{}^*},$$
$$\tau_4 = \frac{\gamma R(z)\left(\sum_{j=1}^2\sigma_j\left|\alpha_j^2(z)\right|^2\right)(\zeta_3 + i\eta_2)(\zeta_3 - i\eta_2{}^*)}{(\eta_2 + \eta_2{}^*)^2[D(z)(\zeta_3 + i\eta_2)(\zeta_3 - i\eta_2{}^*) + \gamma R(z)\sigma_3|\chi^{(3)}(z)|^2]}, \quad \kappa_4^{(3)} = \tau_4\frac{\zeta_3 + i\eta_2}{\zeta_3 - i\eta_2{}^*}.$$

The bright 2-soliton is in components 1 and 2, and the dark 2-soliton is in components 3 and 4,

$$q_j = \frac{g_1^{(j)} + g_3^{(j)}}{1 + f_2 + f_4} \quad (\text{for} \quad j = 1,2),$$
$$q_l = \frac{g_0^{(l)}\left(1 + g_2^{(l)} + g_4^{(l)}\right)}{1 + f_2 + f_4} \quad (\text{for} \quad l = 3,4), \tag{A2}$$

where

$$g_1{}^{(j)} = \alpha_1^{(j)}(z)e^{\theta_1} + \alpha_2^{(j)}(z)e^{\theta_2},$$
$$g_3{}^{(j)} = l_{j1}e^{\theta_1+\theta_1{}^*+\theta_2} + l_{j2}e^{\theta_1+\theta_2+\theta_2{}^*},$$
$$g_0{}^{(l)} = \chi^{(l)}(z)e^{\phi(l)},$$

$$g_2{}^{(l)} = \kappa_1^{(l)}e^{\theta_1+\theta_1{}^*} + \kappa_2^{(l)}e^{\theta_2+\theta_1{}^*} + \kappa_3^{(l)}e^{\theta_1+\theta_2{}^*} + \kappa_4^{(l)}e^{\theta_2+\theta_2{}^*},$$
$$g_4{}^{(l)} = \rho^{(l)}e^{\theta_1+\theta_1{}^*+\theta_2+\theta_2{}^*},$$
$$f_2 = \tau_1e^{\theta_1+\theta_1{}^*} + \tau_2e^{\theta_2+\theta_1{}^*} + \tau_3e^{\theta_1+\theta_2{}^*} + \tau_4e^{\theta_2+\theta_2{}^*},$$
$$f_4 = \varrho e^{\theta_1+\theta_1{}^*+\theta_2+\theta_2{}^*},$$

$$\theta_1 = i\frac{\eta_1{}^2}{2}\int D(z)dz + \eta_1 t - i\lambda z,$$
$$\theta_2 = i\frac{\eta_2{}^2}{2}\int D(z)dz + \eta_2 t - i\lambda z,$$
$$\phi^{(l)} = -i\frac{\zeta_l{}^2}{2}\int D(z)dz + i\zeta_l t - i\lambda z,$$

$$\alpha_1^{(j)}(z) = \alpha_{1j}\sqrt{\frac{D(z)}{\gamma R(z)}}, \quad \alpha_2^{(j)}(z) = \alpha_{2j}\sqrt{\frac{D(z)}{\gamma R(z)}},$$
$$\chi^{(l)}(z) = \chi^{(l)}\sqrt{\frac{D(z)}{\gamma R(z)}}, \quad \lambda = -\gamma R(z)\sum_{l=3}^{4}\sigma_l|\chi^{(l)}(z)|^2,$$

$$l_{j1} = (\eta_1 - \eta_2)\sqrt{\frac{D(z)}{\gamma R(z)}}\left[\frac{\alpha_{j1}\tau_2}{\eta_1 + \eta_1{}^*} - \frac{\alpha_{j2}\tau_1}{\eta_2 + \eta_1{}^*}\right],$$
$$l_{j2} = (\eta_1 - \eta_2)\sqrt{\frac{D(z)}{\gamma R(z)}}\left[\frac{\alpha_{j1}\tau_4}{\eta_1 + \eta_2{}^*} - \frac{\alpha_{j2}\tau_3}{\eta_2 + \eta_2{}^*}\right],$$

$$\tau_1 = \frac{\gamma R(z)\left(\sum_{j=1}^2\sigma_j\left|\alpha_j^1(z)\right|^2\right)\delta_1\delta_2}{(\eta_1 + \eta_1{}^*)^2\{D(z)\delta_1\delta_2 + \gamma R(z)[\sigma_3|\chi^{(3)}(z)|^2\delta_2 + \sigma_4|\chi^{(4)}(z)|^2\delta_1]\}}, \quad \kappa_1^{(3)} = \tau_1\frac{\zeta_3 + i\eta_1}{\zeta_3 - i\eta_1{}^*}, \quad \kappa_1^{(4)} = \tau_1\frac{\zeta_4 + i\eta_1}{\zeta_4 - i\eta_1{}^*},$$
$$\tau_2 = \frac{\gamma R(z)\left[\sigma_1\alpha_1^1(z)^*\alpha_1^2(z) + \sigma_2\alpha_2^1(z)^*\alpha_2^2(z)\right]\delta_3\delta_4}{(\eta_2 + \eta_1{}^*)^2\{D(z)\delta_3\delta_4 + \gamma R(z)[\sigma_3|\chi^{(3)}(z)|^2\delta_4 + \sigma_4|\chi^{(4)}(z)|^2\delta_3]\}}, \quad \kappa_2^{(3)} = \tau_2\frac{\zeta_3 + i\eta_2}{\zeta_3 - i\eta_1{}^*}, \quad \kappa_2^{(4)} = \tau_2\frac{\zeta_4 + i\eta_2}{\zeta_4 - i\eta_1{}^*},$$
$$\tau_3 = \frac{\gamma R(z)\left[\sigma_1\alpha_1^2(z)^*\alpha_1^1(z) + \sigma_2\alpha_2^2(z)^*\alpha_2^1(z)\right]\delta_5\delta_6}{(\eta_1 + \eta_2{}^*)^2\{D(z)\delta_5\delta_6 + \gamma R(z)[\sigma_3|\chi^{(3)}(z)|^2\delta_6 + \sigma_4|\chi^{(4)}(z)|^2\delta_5]\}}, \quad \kappa_3^{(3)} = \tau_3\frac{\zeta_3 + i\eta_1}{\zeta_3 - i\eta_2{}^*}, \quad \kappa_3^{(4)} = \tau_3\frac{\zeta_4 + i\eta_1}{\zeta_4 - i\eta_2{}^*},$$
$$\tau_4 = \frac{\gamma R(z)\left(\sum_{j=1}^2\sigma_j\left|\alpha_j^2(z)\right|^2\right)\delta_7\delta_8}{(\eta_2 + \eta_2{}^*)^2\{D(z)\delta_7\delta_8 + \gamma R(z)[\sigma_3|\chi^{(3)}(z)|^2\delta_8 + \sigma_4|\chi^{(4)}(z)|^2\delta_7]\}}, \quad \kappa_4^{(3)} = \tau_4\frac{\zeta_3 + i\eta_2}{\zeta_3 - i\eta_2{}^*}, \quad \kappa_4^{(4)} = \tau_4\frac{\zeta_4 + i\eta_2}{\zeta_4 - i\eta_2{}^*},$$

$$\delta_1 = |(\zeta_3 + i\eta_1)|^2, \quad \delta_2 = |(\zeta_4 + i\eta_1)|^2, \quad \delta_3 = (\zeta_3 + i\eta_2)(\zeta_3 - i\eta_1{}^*), \quad \delta_4 = (\zeta_4 + i\eta_2)(\zeta_4 - i\eta_1{}^*),$$
$$\delta_5 = (\zeta_3 + i\eta_1)(\zeta_3 - i\eta_2{}^*), \quad \delta_6 = (\zeta_4 + i\eta_1)(\zeta_4 - i\eta_2{}^*), \quad \delta_7 = |(\zeta_3 + i\eta_2)|^2, \quad \delta_8 = |(\zeta_4 + i\eta_2)|^2,$$
$$\varrho = |\eta_1 - \eta_2|^2\left[\frac{\tau_1\tau_4}{|\eta_1 + \eta_2|^2} - \frac{\tau_2\tau_3}{(\eta_2 + \eta_2{}^*)(\eta_1 + \eta_1{}^*)}\right], \quad \rho^{(3)} = \varrho\frac{\delta_5(\zeta_3 + i\eta_2)^2}{\delta_3(\zeta_3 - i\eta_2{}^*)}, \quad \rho^{(4)} = \varrho\frac{\delta_6(\zeta_4 + i\eta_2)}{\delta_4(\zeta_4 - i\eta_2{}^*)^2}.$$

[1] A. Hasegawa and F. Tappert, Appl. Phys. Lett. **23**, 142 (1973); **23**, 171 (1973).

[2] L. F. Mollenauer, R. H. Stolen, and J. P. Gordon, Phys. Rev. Lett. **45**, 1095 (1980).

[3] D. Foursa and P. Emplit, Electron. Lett. **32**, 919 (1996).
[4] G. P. Agarwal, *Nonlinear Fiber Optics* (Academic, London, 1995).
[5] Y. S. Kivshar and B. Luthar-Davies, Phys. Rep. **298**, 81 (1998).
[6] H. Kumar, A. Malik, and F. Chand, Pramana J. Phys. **80**, 361 (2013).
[7] V. N. Serkin and A. Hasegawa, Phys. Rev. Lett. **85**, 4502 (2000).
[8] V. N. Serkin and A. Hasegawa, IEEE J. Sel. Top. Quantum Electron. **8**, 418 (2002).
[9] V. N. Serkin, A. Hasegawa, and T. L. Belyaeva, Phys. Rev. Lett. **98**, 074102 (2007).
[10] V. N. Serkin, A. Hasegawa, and T. L. Belyaeva, Phys. Rev. A **81**, 023610 (2010).
[11] W. J. Liu and B. Tian, Opt. Quant. Electron. **43**, 147 (2012).
[12] C. C. Mak, K. W. Chow, and K. Nakkeeran, J. Phys. Soc. Jpn. **74**, 1449 (2005).
[13] R. Ganapathy, K. Porsezian, A. Hasegawa, and V. N. Serkin, IEEE J. Quant. Electron. **44**, 383 (2008).
[14] X. G. He, D. Zhao, L. Li, and H. G. Luo, Phys. Rev. E **79**, 056610 (2009).
[15] Z. Y. Yang, L. C. Zhao, T. Zhang, X. Q. Feng, and R. H. Yue, Phys. Rev. E **83**, 066602 (2011).
[16] C. Liu, Z. Y. Yang, M. Zhang, T. Zhang, Y. Wen-Li, and R. H. Yue, Commun. Theor. Phys. **59**, 703 (2013).
[17] H. Sakaguchi and B. A. Malomed, Phys. Rev. E **72**, 046610 (2005).
[18] S. V. Manakov, Zh. Eksp. Teor. Fiz. **65**, 505 (1973) [Sov. Phys. JETP **38**, 248 (1974)].
[19] V. V. Afanasjev and V. N. Serkin, *Interaction of Vector Solitons, Nonlinear Guided Wave Phenomena*, Vol. 15 of 1993 OSA Technical Digest Series (Optical Society of America, Washington, DC, 1993), paper TuB13; Sov. Lightwave Commun. **3**, 101 (1993).
[20] R. Radhakrishnan and M. Lakshmanan, J. Phys. A **28**, 2683 (1995); **40**, 13023 (2007).
[21] S. C. Tsang, K. Nakkeeran, B. A. Malomed, and K. W. Chow, Opt. Commun. **249**, 117 (2005).
[22] S. C. Tsang, K. S. Chiang, and K. W. Chow, Opt. Commun. **229**, 431 (2004).
[23] R. Radhakrishnan, M. Lakshmanan, and J. Hietarinta, Phys. Rev. E **56**, 2213 (1997).
[24] A. P. Sheppard and Y. S. Kivshar, Phys. Rev. E **55**, 4773 (1997).
[25] M. Soljacic, K. Steiglitz, S. M. Sears, M. Segev, M. H. Jakubowski, and R. Squier, Phys. Rev. Lett. **90**, 254102 (2003).
[26] Y. Jiang, B. Tian, W. J. Liu, K. Sun, M. Li, and P. Wang, Phys. Rev. E **85**, 036605 (2012).
[27] L. G. Si, W. X. Yang, X. Y. Lü, J. H. Li, and X. X. Yang, Eur. Phys. J. D **55**, 161 (2009).
[28] T. Kanna, M. Lakshmanan, P. T. Dinda, and N. Akhmediev, Phys. Rev. E **73**, 026604 (2006).
[29] W. P. Zhong and M. Belic, Phys. Rev. E **82**, 047601 (2010).
[30] L. Han, Y. Huang, and H. Liu, Commun. Nonlin. Sci. Numer. Simulat. **19**, 3063 (2014).
[31] R. Hirota, in *Solitons*, edited by R. K. Bullough and P. J. Coudrey (Springer, Berlin, 1980), p. 157; Prog. Theor. Phys. **52**, 1498 (1974); J. Hietarinta, J. Math. Phys. **29**, 628 (1988).
[32] S. Nandy, D. Sarma, A. Barthakur, and A. Borah, Commun. Nonlin. Sci. Numer. Simulat. **15**, 3386 (2010).
[33] K. W. Chow, Wave Motion **35**, 71 (2002); K. W. Chow and D. W. C. Lai, Phys. Rev. E **65**, 026613 (2002).
[34] M. J. Ablowitz, D. J. Kaup, A. C. Newell, and M. Segur, Stud. Appl. Math. **LIII**, 249 (1974).